

SUBSTORM OBSERVATIONS OF THE MAIN IN APATITY DURING St. PATRICK'S DAY GEOMAGNETIC STORMS IN 2013 AND 2015

I.V. Despirak¹, B.V. Kozelov¹, V. Guineva²

¹*Polar Geophysical Institute, Apatity, Russia*

²*Space Research and Technology Institute (SRTI), Stara Zagora Department, BAS, P.O. Box 73, 6000
Stara Zagora, Bulgaria*

e-mails: despirak@gmail.com, boris.kozelov@gmail.com, v_guineva@yahoo.com

Abstract. This study presents an analysis of the ground-based observations of the auroral disturbances during two St. Patrick's Day geomagnetic storms on March 17, 2013 and 2015. The first event on 17 March 2015 is the so-called "St. Patrick's Day 2015 Event". This is the principal event covering the interval from 15 to 18 March 2015, in which solar eruptive phenomena (a long-enduring C9-class solar flare and associated CME(s) on 15 March) and a strong geomagnetic storm on 16-18 March (Max. D_{st} was -228 nT) were reported. This magnetic storm is the largest one observed in the current solar cycle. The second event is the period on 17-18 March 2013 when a strong geomagnetic storm (the D_{st} index \sim -140 nT) was developed. This storm was caused by magnetic cloud (15 UT, 17 March – 6 UT, 18 March 2013) in the solar wind. Object of our study were the substorms observed during these periods. Observations of the Multiscale Aurora Imaging Network (MAIN) in Apatity have been used. Solar wind and interplanetary magnetic field parameters were taken from OMNI data base. Substorm onset time and the subsequent development were verified by data of IMAGE magnetometers network and by data of the all-sky camera at Apatity. The particularities in the behaviours of substorms connected with different storms during these two interesting strongly disturbed periods are discussed.

Introduction

It is known that geomagnetic storms may be caused by the following types of solar wind: ICME including Sheath region and body of ICME (magnetic cloud, MC) and CIR- region (e.g. [1]). It should be noted that there are differences between storms generated by Sheath, MC and CIR (in intensity, recovery phase duration, etc.) (e.g., [2], [3], [4]). However, there are also more complicated storm cases, when the magnetic storms are caused by several sources in the solar wind, coming consecutively one after the other or partly overlapping. Such case, for example, is one event of strong geomagnetic activity on 7-17 March 2012 which was examined recently (e.g. [5]).

In our work we considered two strong storm cases during March 2013 and March 2015. The geomagnetic storm occurred on 17–19 March 2015 was the record in strength over the past ten years. It was the strongest storm in the 24th solar cycle. It was called "St. Patrick's Day 2015 Event". The second event is the period 17-18 March 2013 when a strong geomagnetic storm was developed. On 17.03.2013 a magnetic cloud passed by the Earth, and a geomagnetic storm with $D_{ST} \sim$ -140 nT developed.

We considered substorms observations during these two disturbed periods, in March 2013 and March 2015, in Apatity. We have measurements from the Multiscale Aurora Imaging Network (MAIN) in Apatity during these two St. Patrick's Day geomagnetic storms. Below two examples of substorms observations during the first and the second storms are presented.

Data

Measurements from the Multiscale Aurora Imaging Network (MAIN) in Apatity during the strongly disturbed periods in March 2013 and in March 2015 have been used. Substorm presence was verified by ground-based data of IMAGE magnetometers network (using the meridional chain NUR-NAL). Solar wind and interplanetary magnetic field parameters were taken from the 1-min sampled OMNI data base (spacecraft-interspersed, near Earth data) of the Coordinated Data Analysis Website (<http://cdaweb.gsfc.nasa.gov/cgi-bin/eval2.cgi>). To study the substorm development data from the Apatity all-sky camera (images and keograms) and the Guppy F-044C (GC) camera with a field of view \sim 67° (keograms) were used.

Observations

Case 1: 17 March 2015

The time interval 17 – 20 March 2015 is one of the strong geomagnetic storm of the periods of the ascending phase of SC24. An overview of the interplanetary conditions during this examined period is presented in Fig. 1.

Fig. 1 shows the solar wind conditions taken from the OMNI database for the period 16- 27 March, 2015. A severe geomagnetic storm (G4) developed during this time. It was the result of a pair of CME's which left the Sun on 15 March 2015, may be unexpectedly combined spreading towards Earth and formed a large shock front crossing

the Earth orbit. In 4:45 UT a geomagnetic sudden impulse was registered in all stations of the IMAGE magnetometers network which indicated that the shock wave formed by the CME swept past our planet. It coincides with the storm sudden commencement when SYM/H index jumped from 16 to 66 nT. A Magnetic cloud passed the Earth and just after it a HSS superposed and contributed to the storm duration. D_{ST} index reached the value -228 nT in 22:47 UT on 17 March 2015. The solar wind magnetic cloud (MC) and the high speed stream (HSS) regions are shown by shaded red (to the left) and green (to the right) rectangles.

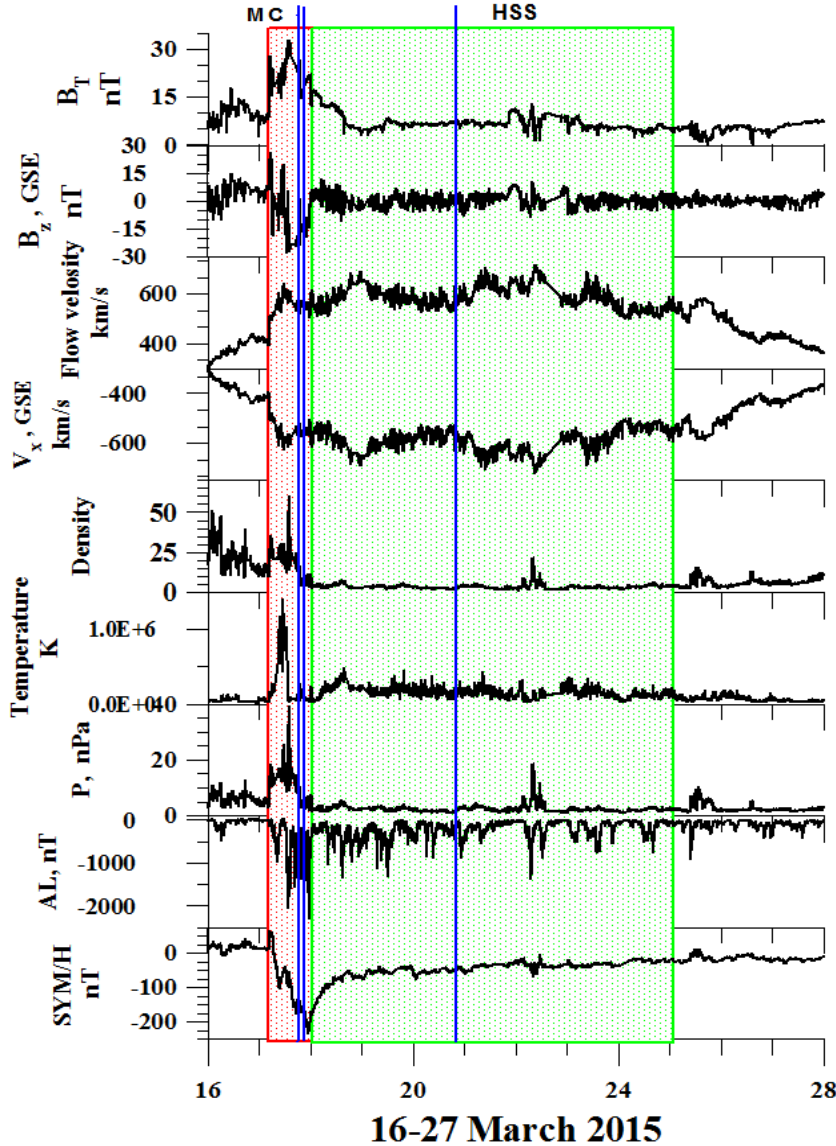


Figure 1. Solar wind and IMF parameters, AL and SYM/H indices on March 16-27, 2015. Top-down: magnetic field magnitude and the IMF B_z component, the stream velocity V , the X component of the solar wind velocity, the density N , the temperature T , the solar wind dynamic pressure P , the geomagnetic index AL and the index SYM/H. The time period of the magnetic cloud (MC) and high speed stream (HSS) are marked as red and green crosshatched areas, respectively. The onset times of 3 substorms are marked by blue solid vertical lines.

Under these highly disturbed conditions, 8 substorms were identified by the all-sky camera in Apatity: two of them occurred during the main storm phase, one – in the vicinity of the SYM/H peak, on 17 March 2015, five - in the recovery phase and in the late recovery phase of the storm, on 18 and 20 March 2015.

Below an example of substorm observations is presented - one substorm event during the storm main phase, in 17:36 UT on 17 March 2015.

In Fig. 2 one substorm development during co-called “St. Patrick’s Day 2015 Event” was presented. Development of the substorm on 17 March 2015 in 17:36:40 by chosen all-sky images (top panel), by all-sky keogram (left bottom panel) and Guppy (GC) camera keograms (right bottom panels). The world directions are marked in the first image; the universal time is written above each image. The substorm was observed during the main phase of the severe geomagnetic storm on 17 March 2015. The SYM/H value at the moment of substorm onset was ~ -163 nT.

As seen in figure substorm auroras appeared in the South part of the field of view in 17:36:40 UT. For some minutes auroras stayed in the South part of the field of view. In 17:42 UT a fast motion towards North was observed and in 17:45:30 UT the auroras occupied the whole field of view.

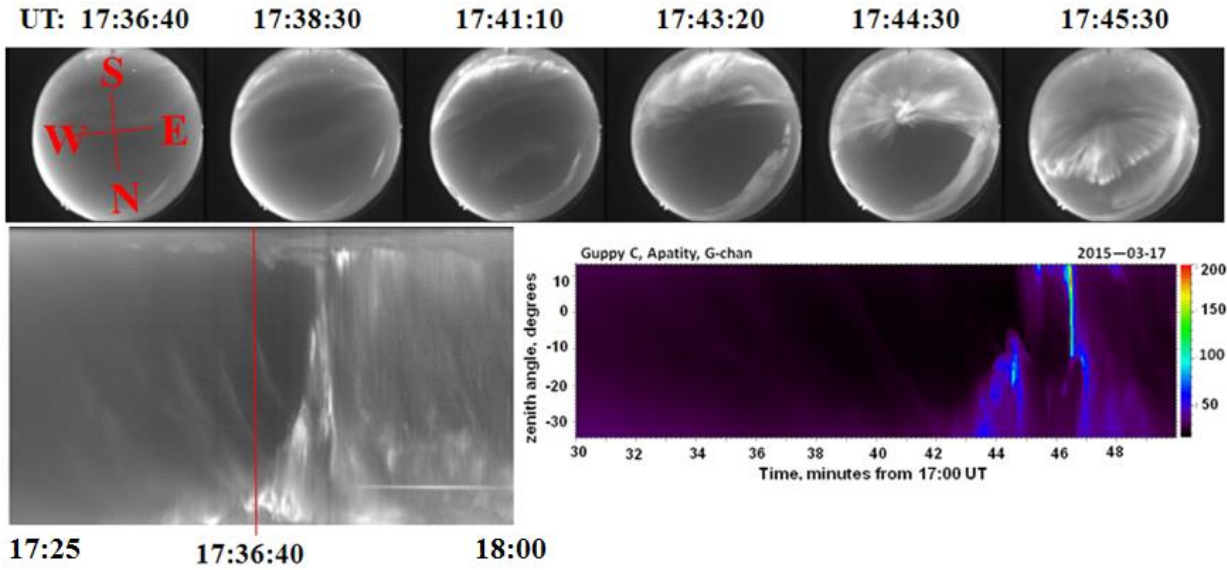


Figure 2. Development of the substorm on 17 March 2015 in 17:36:40 by chosen all-sky images (top panel), by all-sky keogram (left bottom panel) and Guppy (GC) camera keograms (right bottom panels).

In the GC keogram, the substorm auroras are seen from 17:42:30 UT at the South part of the field of view, at 35° from zenith, due to the fast movement to North. Then a maximal intensity of 200 rel. units was observed about 17:46:25 UT.

Case 2: 17 March 2013

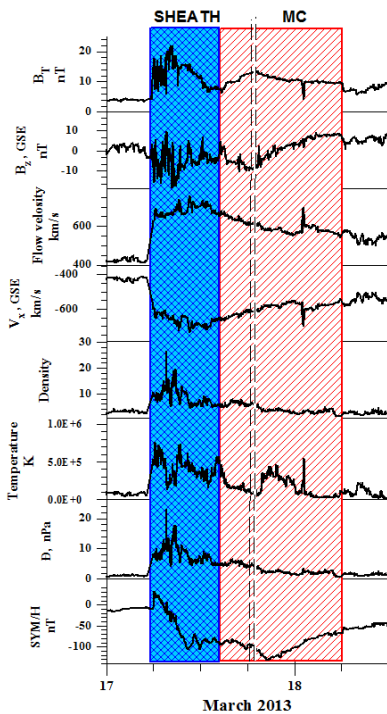


Figure 3. Solar wind and IMF parameters and SYM/H index on March 17-18, 2013. The onset times of two substorms are marked by dashed black vertical lines.

The solar wind conditions taken from the OMNI database for the magnetic cloud on 17-18 March 2013 are presented in Fig. 3. The time period of the magnetic cloud (MC) (15 UT, 17 March – 6 UT, 18 March 2013) and the region of interaction of MC with the undisturbed solar wind (Sheath) (06-15 UT on 17 March 2013) are marked as red and blue crosshatched areas, respectively. A geomagnetic storm developed during this time. The D_{ST} index reached ~ -140 nT. Under these highly disturbed conditions, during the main phase of the storm, two substorms were observed at 18:26 UT and 18:39 UT, 17 March 2013 by the all-sky camera in Apatity. The onset times of these substorms are marked by black dashed vertical lines.

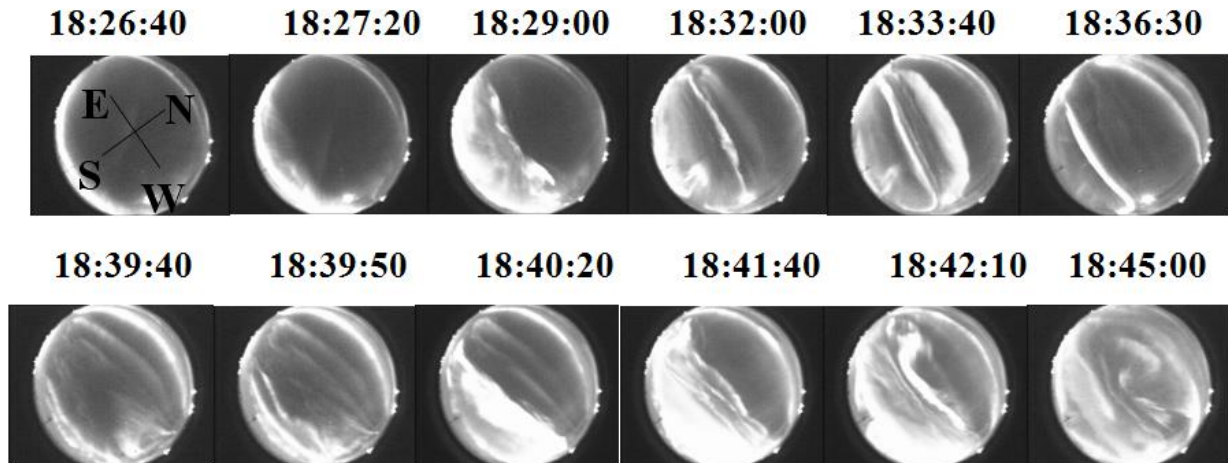


Figure 4. Development of the two substorms on 17 March 2013 by chosen all-sky images.

Fig. 4 shows the dynamics of auroras according to the all-sky camera data during substorms on 17 March 2013. The all-sky camera in Apatity registered the substorm onset at 18:26:40 UT and the second substorm intensification at 18:39:40 UT. The top panel shows some all-sky camera images taken during the first substorm, the bottom panel shows images from the second substorm. The world directions are marked in the first image; the universal time is written above each image. The substorm beginning to the South from the station, the arcs movement to the North, reaching the station zenith (18:32 UT) and surpassing it are seen. The second intensification at Apatity begins with an equatorial arc burst at 18:39:40 UT. After that, auroras move toward zenith, reach it at 18:41:40, and continue moving northward.

Conclusions

1. Substorms, originated during the main storm phase or near the SYM/H minimum in the recovery phase, occurred to the South of Apatity (63.86°N GMLat.), and substorm auroras expanded in North direction.
2. For substorms during the recovery phase or the late recovery phase, auroras were observed near the station zenith or to the North of the Apatity station, and their motion from North to South was registered.
3. The boundary between both types of substorms in terms of SYM/H index is in the range 40-50 nT.
4. The maximal relative intensity of the substorm features in the camera field of view is considerably larger during the substorms arised to the South from Apatity.

Acknowledgments. This study was supported by Program No 7 of the Presidium of RAS. The study is part of a joint Russian - Bulgarian Project “The influence of solar activity and solar wind streams on the magnetospheric disturbances, particle precipitations and auroral emissions” of PGI RAS and IKIT-BAS under the Fundamental Space Research Program between RAS and BAS.

References

1. Gonzalez W.D., A.L.C. Gonzalez, B.T. Tsurutani (1990), Dual-peek solar cycle distribution of intense geomagnetic storms. *Planet. Space Sci.* 38, 181-187.
2. Huttunen K.E.J., H.E.J. Koskinen, A. Karinen, K. Mursula (2006) Asymmetric development of magnetospheric storms during magnetic clouds and sheath regions. *Geophys. Res. Lett.* 33, L06107, doi:10.1029/2005GL024894.
3. Pulkkinen T.I., N.Y. Ganushkina, E.I. Tanskanen, M. Kubyshkina, G.D. Reeves, M.F. Thomsen, C.T. Russel, H.J. Singer, J.A. Slavin, J. Gjerloev (2006), Magnetospheric current systems during stormtime sawtooth events, *J. Geophys. Res.* 111, A11S17, doi:10.1029/2006JA011627.
4. Yermolaev Yu.I., M.Yu. Yermolaev (2006), Statistic study on the geomagnetic storm effectiveness of solar and interplanetary events. *Adv. Space Res.* 37, 11 75-1181.
5. Tsurutani B.T., E. Echer, K. Shibata, O.P. Verkhoglyadova, A.J. Mannucci, W.D. Gonzalez, J.U. Kozyra, M. Pätzold (2014), The interplanetary causes of geomagnetic activity during the 7–17 March 2012 interval: a CAUSES II overview. *J. Space Weather Space Clim.*, 4, A02, DOI: 10.1051/swsc/2013056.